RADIATION RESEARCH **164**, 518–522 (2005)
0033-7587/05 $15.00

Immunofluorescence Detection of Clustered γ-H2AX Foci Induced by HZE-Particle Radiation

N. Desai,[a] E. Davis,[b] P. O'Neill,[b] M. Durante,[c] F. A. Cucinotta[d,1] and H. Wu[d]

[a] *Wyle Laboratories, Houston, Texas;* [b] *Medical Research Council, Radiation and Genome Stability Unit, Harwell, Didcot, United Kingdom;* [c] *Department of Physics, University of Naples, Naples, Italy; and* [d] *NASA Johnson Space Center, Houston, Texas*

Desai, N., Davis, E., O'Neill, P., Durante, M., Cucinotta, F. A. and Wu, H. Immunofluorescence Detection of Clustered γ-H2AX Foci Induced by HZE-Particle Radiation. ***Radiat. Res.*** **164, 518–522 (2005).**

We studied the spatial and temporal distributions of foci of the phosphorylated form of the histone protein H2AX (γ-H2AX), which is known to be activated by double-strand breaks after irradiation of human fibroblast cells with high-energy silicon (54 keV/μm) and iron (176 keV/μm) ions. Here we present data obtained with the ion path parallel to a monolayer of human fibroblast cells that leads to γ-H2AX aggregates in the shape of streaks stretching over several micrometers in an *x*/*y* plane, thus enabling the analysis of the fluorescence distributions along the ion trajectories. Qualitative analyses of these distributions provide insights into DNA damage processing kinetics for high charge and energy (HZE) ions, including evidence of increased clustering of DNA damage and slower processing with increasing LET.

INTRODUCTION

The biological effects of high charge and energy (HZE) ions are a concern for astronaut health during space missions (*1*). Track structure is known to be a critical determinant of the biological effectiveness of charged-particle radiation (*1–3*). Although there is convincing evidence that the extremely large localized energy deposition by HZE ions leads to particularly complex types of damage (*4–7*), the spatial distribution of damage in subcellular dimensions had not been visualized until recently. Jakob and colleagues have demonstrated using appropriate immunofluorescence staining techniques based on antibodies against proteins involved in the DNA damage response, e.g. CDKN1A (p21) and MRE11B, that the positions of foci can be clearly assigned to the locations of individual particle traversals (*8, 9*). However, irradiation of cell samples with the particle beam perpendicular to the monolayer of cells results in individual foci and clusters but not the distribution of foci over long segments of an ion's trajectory through a cell nucleus. By using a ''parallel'' radiation geometry where the beam is applied at a very small angle (less than 5°) with respect to the plane of cells, allows detection of the biological response along the particle trajectory has been made possible. The radiation geometry allows detection of the nonrandom pattern of foci (*9*).

Recently an immunofluorescence technique using an antibody probe against the phosphorylated form of the variant histone protein H2AX (γ-H2AX) has been used to detect DNA DSBs in irradiated cells at low doses (*10–14*). H2AX is known to be phosphorylated rapidly in response to DNA DSBs, leading to the formation of nuclear foci visualized by immunocytochemical detection of γ-H2AX (*10–12*). Analysis of these fluorescent markers allows for a qualitative measure of DNA damage; however, its use as a quantitative tool for describing the spatial distribution of DNA damage is of interest (*13, 15*). By using a modified irradiation geometry with the beam parallel to a monolayer of cells and probing for γ-H2AX, we observed the formation of foci along the particle trajectories through cell nuclei. We offer evidence of differential DNA damage induction and processing kinetics for distinct HZE ions as represented by the spatial and temporal characteristics of γ-H2AX clusters.

MATERIALS AND METHODS

Cell Culture and Irradiation

Confluent normal human foreskin fibroblasts (AG1522B) were cultured in chamber slide flasks (Nalgene) at 37°C in a humidified atmosphere of 95% air/5% CO_2 in DMEM containing 10% fetal calf serum. Cells were irradiated with either iron or silicon ions with the beam parallel to the monolayer of cells. We employed heavy-ion beams accelerated at the NASA Space Radiation Laboratory (NSRL) at the Brookhaven National Laboratory (BNL) in New York at several doses with average dose rates of about 0.5 Gy/min.

Immunofluorescence and Microscopy

After irradiation, cells were fixed with 2% paraformaldehyde in PBS at 10 min or 1, 5 or 24 h postirradiation and were subsequently immunostained for γ-H2AX as described previously (*14*). Labeled cell preparations were then examined with a fluorescence microscope equipped

[1] Address for correspondence: NASA Johnson Space Center, Mail Code SK, Houston, TX 77058; e-mail: francis.a.cucinotta@nasa.gov.

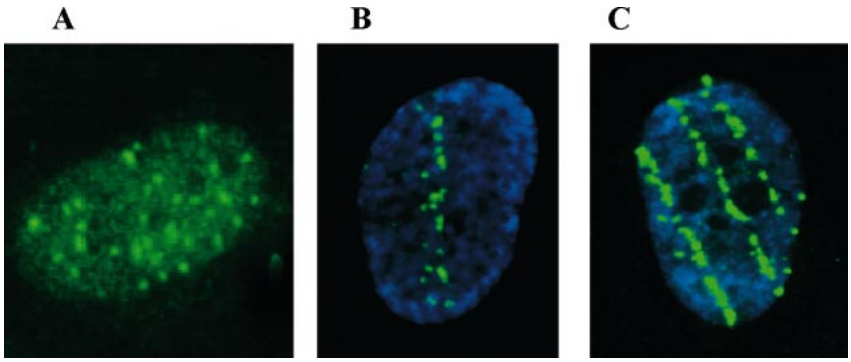

FIG. 1. Formation of fluorescent γ-H2AX clusters in irradiated human fibroblasts at 10 min postirradiation with (panel A) 2 Gy of γ rays, (panel B) 0.5 Gy of 54 keV/μm silicon ions, or (panel C) 0.5 Gy of 176 keV/μm iron ions. Each panel shows the DAPI-stained nucleus (blue) and anti-γ-H2AX antibody (green).

with a CCD imaging system. Images were captured using the accompanying image processing software from Cytovision with bandpass filter sets allowing the visualization of the Alexa 488 dye for γ-H2AX identification and DAPI as the nuclear counterstain. At least 200 nuclei were scored for each data point.

RESULTS AND DISCUSSION

The spatial distribution of DNA lesions within the cell nucleus produced by charged particles depends on the ion track structure as well as the random nature of the ion impact parameter relative to the cell nucleus and the Poisson distribution of the number of hits per cell (*2, 3*). To determine how the patterns of DNA damage change with ion track structure, we compared γ-H2AX foci from cells exposed to silicon ions (581 MeV/nucleon; 54 keV/μm) to those obtained from cells exposed to higher-LET iron ions (600 MeV/nucleon; 176 keV/μm) at doses of 0.5 Gy. At these doses, an average of about six silicon ions or two iron ions intersect each cell nucleus. After parallel irradiation of monolayers of human fibroblast cells with iron or silicon ions and immunostaining using antibodies against γ-H2AX, we observed fluorescent ''streaks'' of γ-H2AX foci inside the cell nuclei (Fig. 1B and C). These fluorescent streaks were visible as early as 10 min postirradiation. Sham-irradiated control fibroblasts lacked this type of γ-H2AX staining pattern (not shown). The observed patterns of clustered foci were almost parallel in all cell nuclei displaying streak-like patterns, most likely revealing the ion trajectory through the cell nuclei. These streaking patterns were often found to extend over two to three neighboring nuclei.

The staining pattern of γ-H2AX we observed was not homogeneous or continuous but instead displayed grainy substructures or fluorescent clusters with gaps between the clusters along the presumed ion trajectory (Fig. 2A). Fluorescent clusters and isolated foci were distinguished by eye, assuming that a fluorescent cluster included a series of foci extending over one-half or more of the cell nucleus, indicating a likely ion traversal. Only fluorescent clusters were scored in the quantitative analysis presented below. Larger gaps were attributed to regions of the cell nucleus contain-

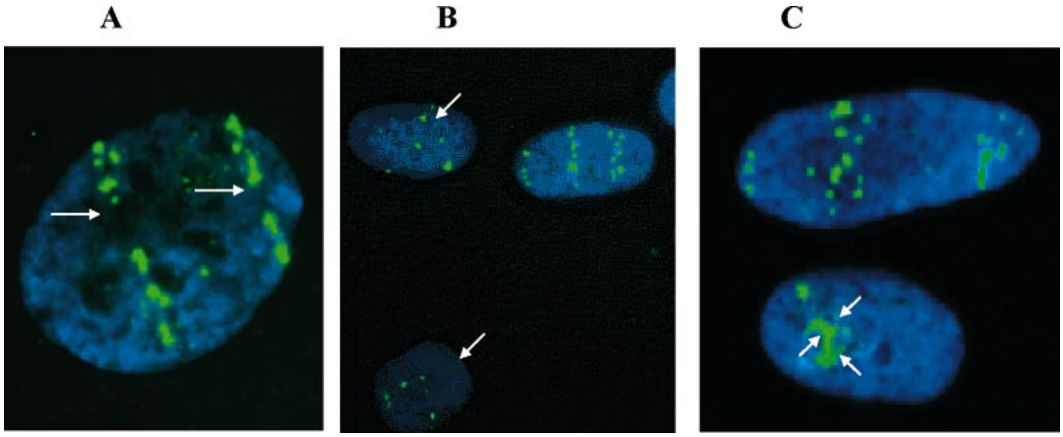

FIG. 2. Normal human fibroblasts after irradiation. Panel A: Irradiated with 0.5 Gy of iron ions and fixed 10 min postirradiation. Arrows show areas lacking γ-H2AX staining in regions most probably consisting of nucleoli as seen by the lack of DNA staining. Panel B: Irradiated with 0.5 Gy of silicon ions and fixed 10 min postirradiation. Arrows indicate cells that may not have been traversed by a primary beam, displaying a random distribution of fluorescent clusters. Panel C: Irradiated with 1.7 Gy of iron ions fixed 5 h after irradiation. Arrows indicate areas of possible DNA DSB clustering.

ing little DNA such as the pockets of nucleoli distributed randomly throughout the nuclei (*9*). The γ-H2AX fluorescent clusters were not limited to regions of ion traversal but were also observed to appear randomly as nuclear foci in some cells. In fact, some cell nuclei exclusively contained such discrete γ-H2AX foci and possibly were not traversed by the so-called ion core (*2, 3*) (Fig. 2B). Our analysis of γ-H2AX clusters produced by silicon and iron ions reveals a clear distinction between the two ions. Iron-particle irradiation resulted in γ-H2AX fluorescent clusters that were much wider on average (Fig. 1C) than those produced by silicon ions, and the fluorescent clusters produced by silicon ions appeared to be less dense along the length of each cluster (Fig. 1B).

We also performed a relative quantitative analysis to compare the effects of silicon and iron ions on the extent of DNA damage. The mean number of fluorescent clusters in about 200 cells (scored by eye) was used as a quantitative measure to compare the initial DNA damage induced by iron and silicon ions in human fibroblasts. Though some clusters were larger than others, each was assessed as a single unit, regardless of its size. Furthermore, all fluorescent clusters were included in the analysis, even those in which no apparent ion trajectory was found. Our data indicated a significantly larger number of fluorescent clusters (approximately threefold greater) in fibroblasts irradiated with 0.5 Gy of iron particles than in cells receiving the same absorbed dose of silicon ions (Fig. 3A). Because on average there are about three times more silicon-ion tracks than iron-particle tracks per cell nucleus at this dose, our results indicate that iron ions have a greater effectiveness per particle for producing fluorescent clusters. Interestingly, the percentage of cells with clearly visible γ-H2AX streaks at 10 min postirradiation was similar for both iron-particle- and silicon-ion-irradiated fibroblasts, with approximately one in two cells displaying fluorescent streaks. Our results are distinct from those of a previous study using fluorescence staining of MRE11 protein in normal human fibroblasts along particle trajectories produced by heavy ions of varying LET, which did not display any differential characteristics in terms of width and/or substructure (*9*).

The gradual dissolution of the γ-H2AX fluorescence signal as DNA repair progresses has been shown to be a useful predictor of DSB rejoining kinetics (*15*). We applied similar methods in our study to examine the disappearance of γ-H2AX fluorescent clusters over time. Fibroblasts irradiated with 0.5 Gy of iron or silicon ions were fixed with paraformaldehyde at 10 min and 1, 5 and 24 h after exposure. We calculated the percentage of cell nuclei that still contained γ-H2AX streaks across the nuclear area as a relative measure of DNA repair. Ten minutes after irradiation with both silicon and iron ions, almost 50% of cells had γ-H2AX streaks (49.0 ± 3.7 and 50.4 ± 4.6% for silicon and iron ions, respectively). However, with increasing time postirradiation, the decrease in the percentage of cells with tracks was slower in cells exposed to iron particles, with a twofold

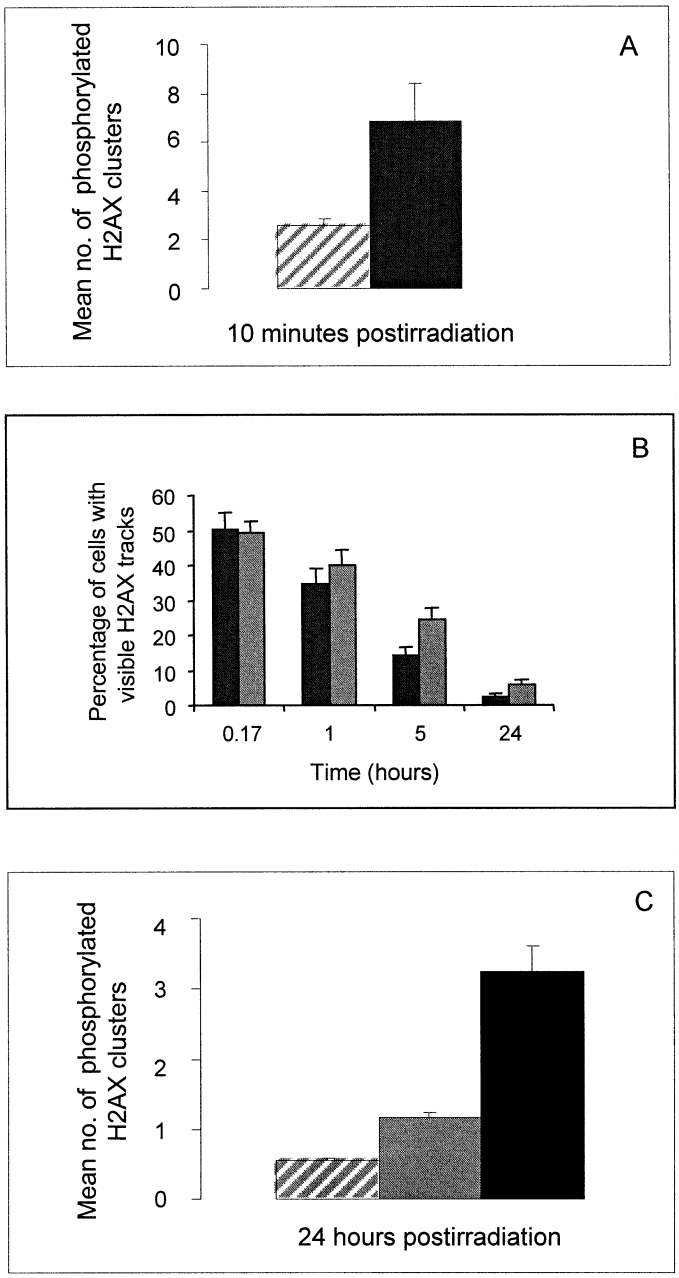

FIG. 3. Panel A: Relative amount of H2AX phosphorylation in human fibroblasts irradiated with iron and silicon ions and fixed 10 min after irradiation. The mean numbers of fluorescent γ-H2AX clusters were measured in about 200 cells after exposure to 0.5 Gy silicon (shaded bar) or iron (solid bar) ions with standard errors shown. Panel B: Time course of DNA repair after irradiation represented by fluorescent γ-H2AX streaks. The percentage of cells with visible streaks was used as a relative measure of DNA repair after irradiation. Bars indicate relative DNA rejoining after exposure to 0.5 Gy of silicon (solid bars) or iron (shaded bars) ions with standard errors shown. Panel C: Residual DNA damage after 24 h repair. Human fibroblasts were irradiated with 0.5 Gy silicon ions (striped bar), 0.5 Gy iron ions (shaded bar), or 1.7 Gy iron ions (solid bar), and the relative amount of residual DNA damage was calculated by measuring the mean number of fluorescent γ-H2AX clusters visible at 24 h postirradiation with standard errors shown.

higher percentage of cells with streaks at 24 h postirradiation compared to cells exposed to silicon ions (2.3 ± 0.9 and 5.8 ± 1.3% for silicon and iron ions, respectively). These results indicated that the higher-LET iron ions produced slower rejoining of DSBs, resulting in a higher number of residual DNA breaks compared to those seen after exposure to silicon ions. To confirm this, we measured the absolute number of γ-H2AX fluorescent clusters in cell nuclei 24 h after irradiation with 0.5 Gy of either iron or silicon ions. At 24 h postirradiation, we observed a random dissolution of the γ-H2AX signal along the particle tracks with a homogeneous distribution of distinct γ-H2AX fluorescent clusters dispersed arbitrarily within cell nuclei. We measured the number of such clusters remaining in cells 24 h after irradiation for a dose of 0.5 Gy of silicon or iron ions and found that cells irradiated with silicon ions contained approximately twofold fewer residual clusters than iron-ion-irradiated cells (Fig. 3C).

A higher frequency of residual γ-H2AX fluorescent clusters was found as the dose was increased. To compare the dose effect on repair kinetics, we irradiated cells with doses of 0.5 and 1.7 Gy of iron particles and measured the relative number of γ-H2AX fluorescent clusters at 24 h after irradiation. The residual number of γ-H2AX clusters was approximately threefold higher in cells exposed to 1.7 Gy than in cell exposed to 0.5 Gy (Fig. 3C). A recent study used γ-H2AX detection to observe the movement of α-particle-induced DSBs; the results suggested that DSBs migrate over large distances (*16*). In an attempt to understand this mechanism, we observed the spatial distribution of γ-H2AX clusters induced by heavy ions by noting track morphology at various times after exposure. Interestingly, we observed that γ-H2AX fluorescent clusters along a track increased in size after irradiation, congregating with other clusters and forming vacant stretches across the initial track structures (Fig. 2C). The spatial pattern of fluorescent streaks was quite stable over several hours despite considerable movement and rotation of the whole nucleus. The clear parallelism of the tracks inside individual nuclei and the alignment of all γ-H2AX streaks within a sample provide indirect evidence that the tracks were generated by individual particles. However, not all γ-H2AX fluorescent clusters were associated with particle trajectories, because some clusters were found to be distributed randomly within nuclei. These isolated clusters reflect the induction of DNA damage by δ rays, secondary nuclear fragments (*1*), and/or possible bystander effects. It is also known that background levels of foci change throughout the cell cycle, peaking in S phase (*17*).

Measurements of DSB yields have suggested that the yields are not strikingly different for various types of radiation; however, some studies suggest that both the spatial distribution of DSBs and rejoining kinetics and fidelity are influenced by radiation quality (*4–6*). Our results indicate that iron ions produce more clustered initial DNA damage in the form of fluorescent clusters than silicon ions with a lower LET at equivalent doses. Analysis of the postirradiation kinetics of γ-H2AX fluorescent clusters revealed a pattern that suggests slower damage processing for higher LET at equivalent doses. γ-H2AX foci persisted in some cells even after a 24-h repair period after exposure to 0.5 Gy of either iron or silicon ions. However, the number of residual foci after exposure to iron ions was significantly higher than after exposure to silicon ions, indicating slower dephosphorylation of γ-H2AX foci and possibly DSB rejoining at higher LET. We observed that the track morphology in iron-particle-irradiated cells was significantly different from that in silicon-ion-irradiated cells, with narrower and shorter clusters observed for the latter. This is in agreement with biophysical models that predict a denser radial substructure of DNA damage for higher-LET particles (*2, 3*). Additionally, we observed changes in track morphology within hours after DSB induction, indicating possible movement of cell nuclei, foci or chromosomal domains. The understanding of such changes presents challenges for future work.

The present method is unable to determine the absolute number of γ-H2AX foci since it cannot resolve breaks that are close together in clusters. Nevertheless, immunofluorescence detection of γ-H2AX is a useful tool in the analysis of high-LET radiation-induced DNA damage, and it may allow us to elucidate whether the nonrandom distributions of DNA breaks produced by high-LET particle tracks have any consequences for their repair and biological effectiveness. It is expected that the use of confocal microscopy and the development of objective imaging scoring criteria will allow for more quantitative analysis to be performed in the future.

ACKNOWLEDGMENTS

This research was supported by the Office of Science (BER), U.S. Department of Energy, Interagency Agreement No. DE-AI03-05ER64088 (FC), and by the NASA Space Radiation Health Program.

Received: July 28, 2004; accepted: March 15, 2005

REFERENCES

1. F. A. Cucinotta, H. Wu, M. R. Shavers and K. George, Radiation dosimetry and biophysical models of space radiation effects. *Gravit. Space Biol. Bull.* **16**, 11–18 (2003).
2. D. T. Goodhead, The initial physical damage produced by ionizing radiations. *Int. J. Radiat. Biol.* **56**, 623–634 (1989).
3. F. A. Cucinotta, H. Nikjoo and D. T. Goodhead, Radial distribution of energy imparted in nanometer volumes from HZE particles. *Radiat. Res.* **153**, 459–468 (2000).
4. T. J. Jenner, C. M. Delara, P. O'Neill and D. L. Stevens, Induction and rejoining of DNA double-strand breaks following γ- and α-irradiation. *Int. J. Radiat. Biol.* **64**, 265–273 (1993).
5. K. M. Prise, M. Pinto, H. C. Newman and B. D. Michael, A review of studies of ionizing radiation-induced double-strand break clustering. *Radiat. Res.* **156**, 572–576 (2001).
6. C. Baumstark-Khan, J. Heilmann and H. Rink, Induction and repair of DNA strand breaks in bovine lens epithelial cells after high LET irradiation. *Adv. Space Res.* **31**, 1583–1591 (2003).

7. H. Hoglund and B. Stenerlow, Induction and rejoining of DNA double-strand breaks in normal human skin fibroblasts after exposure to radiation of different linear energy transfer: Possible roles of track structure and chromatin organization. *Radiat. Res.* **155**, 818–825 (2001).

8. B. Jakob, M. Scholz and G. Taucher-Scholz, Characterization of CDKN1A (p21) binding to sites of heavy-ion-induced damage: Colocalization with proteins involved in DNA repair. *Int. J. Radiat. Biol.* **78**, 75–88 (2002).

9. B. Jakob, M. Scholz and G. Taucher-Scholz, Biological imaging of heavy charged-particle tracks. *Radiat. Res.* **159**, 676–684 (2003).

10. D. R. Pilch, O. A. Sedelnikova, C. Redon, A. Celeste, A. Nussenzweig and W. M. Bonner, Characteristics of gamma-H2AX foci at DNA double-strand breaks sites. *Biochem. Cell Biol.* **81**, 123–129 (2003).

11. E. P. Rogakou, C. Boon, C. Redon and W. M. Bonner, Megabase chromatin domains involved in DNA double-strand breaks *in vivo*. *J. Cell Biol.* **146**, 905–916 (1999).

12. E. P. Rogakou, D. R. Pilch, A. H. Orr, V. S. Ivanova and W. M. Bonner, DNA double-stranded breaks induce histone H2AX phosphorylation on serine 139. *J. Biol. Chem.* **273**, 5858–5868 (1998).

13. K. Rothkamm and M. Lobrich, Evidence for a lack of DNA double-strand break repair in human cells exposed to very low x-ray doses. *Proc. Natl. Acad. Sci. USA* **100**, 5057–5057 (2003).

14. S. Goto, M. Watanabe and F. Yatagi, Delayed cell cycle progression in human lymphoblastoid cells after exposure to high-LET radiation correlates with extremely localized DNA damage. *Radiat. Res.* **158**, 678–686 (2002).

15. P. L. Olive and J. P. Banath, Phosphorylation of histone H2AX as a measure of radiosensitivity. *Int. J. Radiat. Oncol. Biol. Phys.* **58**, 331–335 (2004).

16. J. A. Aten, J. Stap, P. M. Krawczyk, C. H. van Oven, R. A. Hoebe, J. Essers and R. Kanaar, Dynamics of DNA double-strand breaks revealed by clustering of damaged chromosome domains. *Science* **303**, 92–95 (2004).

17. S. H. MacPhail, J. P. Banath, Y. Yu, E. Chu and P. L. Olive, Cell cycle-dependent expression of phosphorylated histone H2AX: Reduced expression in unirradiated but not X-irradiated G_1-phase cells. *Radiat. Res.* **159**, 759–767 (2003).